International Journal of Modern Chemistry, 2020, 12(1): 117-140

Modern Scientific Press

International Journal of Modern Chemistry **ISSN: 2165-0128**

Journal homepage: www.ModernScientificPress.com/Journals/IJMChem.aspx *Florida, USA*

Article

Electrochemical Behavior of Quench-treated Low Carbon Steel in 0.5 H_2SO_4 Medium Containing Simvastatin Drug as Corrosion Inhibitor Using Potentiodynamic and Evans Techniques

Adel H. Ali

Department of Physics, Faculty of Science brunch of Al-tourba, Taiz University, Yemen

* Author to whom correspondence should be addressed; E-Mail: Adelchemst22@gmail.com

Article history: Received 8 August 2020, Revised 25 October 2020, Accepted 26 October 2020, Published 6 November 2020.

Abstract: The rule of this paper is to study the possibility of using the Simvastatin pharmaceutical drug compound as a corrosion inhibitor that can have a decisive effect of decreasing on metallic corrosion rate and adsorbed on the metal surface by using potentiodynamic polarization and Evans techniques. In this regard, we simultaneously present an overview of Simvastatin compound performance, as a corrosion inhibitor in 10% ethanol, 0.5N H_2SO_4 (10A5H), and with presence different concentrations of the drug. The potentiodynamic polarization and Evans technique are studied the LCH in a different medium to clarify the effect of medium on the corrosion processes, and the effect of polarization on the orientation of the inhibitor molecule to the metal surface. The surface examination by scanning electron microscopy (SEM), energy dispersive X-ray (EDX), and atomic force microscopy (AFM). All surface examinations confirm formation thin film adsorbed on the metal surface, which discussed by the mechanism of the adsorption processes on the polarized metal surface.

Keywords: Corrosion Inhibition; Potentiodynamic Polarization; Evans Technique; Mixed Solution (10A5H); Simvastatin Inhibitor; SEM; EDX; AFM.

1. Introduction

Most organic compounds containing nitrogen (N-heterocyclic), sulfur, long carbon chain, or aromatic and oxygen atoms are using a corrosion inhibitors, among them, organic compounds have

Copyright © 2020 by Modern Scientific Press Company, Florida, USA

many advantages such as large molecular size, highly soluble in water, availability, cheap, low toxicity, easy for using and easy production [1]. Natural heterocyclic mixes have been utilized for the corrosion inhibitor on the C-steel [2], copper [3], aluminum [4], and various metals in various aqueous medium [5]. Adsorption of the drug molecules on the metal surface facilitates its inhibition [6]. The investigation of the relations between the adsorption and consumption hindrance is of awesome importance. Heterocyclic mixes have demonstrated more hindrance effectiveness, for C-steel in both HCl [7] and H_2SO_4 arrangements [8]. Numerous authors for the most part, concur that medications are inhibitors that can compete favorably with green inhibition of corrosion and that most medications can be synthesized from natural products. Selection of some medication as corrosion inhibitors due to the followings: (1) drug molecules contain oxygen, sulfur, and nitrogen as active sites, (2) it is environmentally friendly furthermore vital in organic responses and (3) drugs can be easily produced and purified (4) nontoxic compering organic inhibitors. A few medications have been discovered to be great corrosion inhibitors for metals such as Biopolymer gave 86% inhibition efficiency (IE) for Cu in NaCl [9], pyromellitic diimide linked to oxadiazole cycle gave 84.6% IE for mild steel (MS) in HCl [10], 2-mercaptobenzimidazole gave 82% IE for MS in HCl Antidiabetic Drug Janumet gave 88.7% IE for MS in HCl [11]. Januvia gave 79.5 % IE for Zn in HCl [12],Cefuroxime Axetil gave 89.9% IE for Al in HCl [13], Phenytoin sodium gave 79% for MS in HCl [14], Aspirin gave71% IE for MS in H_2SO_4 [15], Septazole gave 84.8% IE for Cu in HCl [16] and Chloroquine diphosphate gave 80% IE for MS in HCl [17]. Study on Structural, Corrosion, and Sensitization Behavior of Ultrafine and Coarse Grain 316 Stainless Steel Processed by Multiaxial Forging and Heat Treatment [18]. Investigating the corrosion of the Heat-Affected Zones (HAZs) of API-X70 pipeline steels in aerated carbonate solution by electrochemical methods [19]. Predictions of corrosion current density and potential by using chemical composition and corrosion cell characteristics in microalloyed pipeline steels [20]. Predictions of toughness and hardness by using chemical composition and tensile properties in microalloyed line pipe steels [21].

The scope of this article is used Simvastatin drug as save corrosion inhibitor for LCH in the acid medium by electrochemical method, and to elucidate the mechanism of corrosion inhibition.

2. Experimental

2.1. Metal Samples

The sample of carbon steel was used in this study that have the chemical composition of the metal sample was determined by using an emission spectrometer, with the aid of ARL quant meter (model 3100-292 IC) and listed in the Table 1.

Copyright © 2020 by Modern Scientific Press Company, Florida, USA

Table 1: Chemical compositions of carbon steel sample

Sample	C%	Mn%	V%	Fe%	Si%
Low; C	0.26	0.77	0.11	98.51	0.35

2.2. Quenching in Oil

The heat treatment regime was used as a quenching in oil. The sample was put in an electric muffle furnace where raising temperature to 920 ºC (Austentizing temperature) through five hours. Then, the sample remains in the furnace for one hour at 920ºC, (Holding time), followed quenching of the sample in oil.

The phase, which formed due to this heat treatment sample is converted from ferretic phase to martensite phase [22]. The steps of this regime are shown diagrammatically in Figure 1.

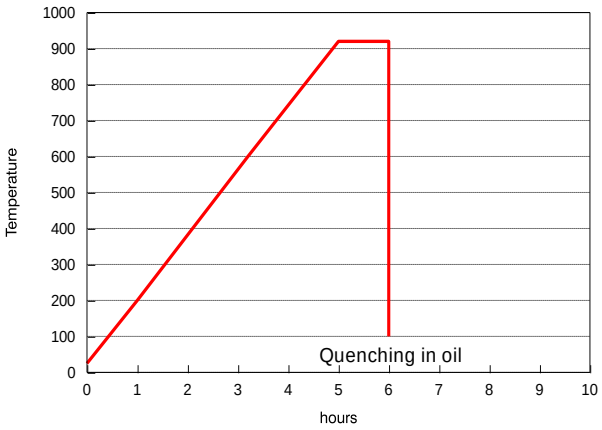


Figure 1: Heat treatment regime

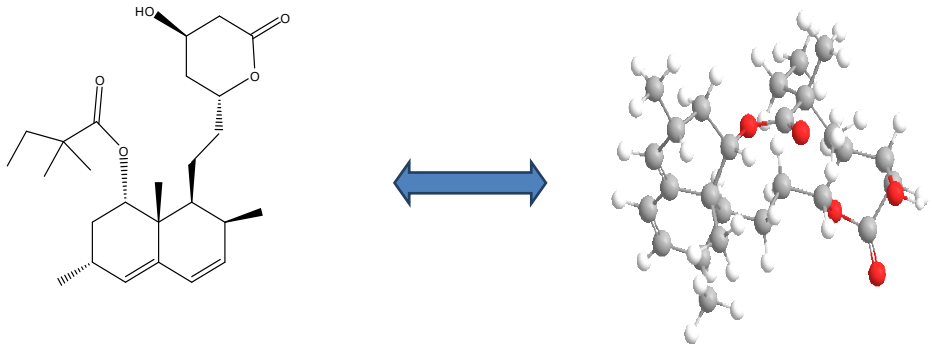
2.3. Preparation of Metal Sample (working electrode)

Working electrode having the surface area, which, exposed to corrosion media is ($1cm^2$) cross-section area, and the rod was weld from one side to a copper wire used for electric connection. The sample was embedded in a glass of just a larger diameter than the sample. Epoxy resin was used to stick the sample to glass tube. These also ensured that a constant cross-sectional area would be exposed to corrosive media, through the experiments. The sample was scraped with SiC polisher sheet coarseness sizes (400, 800 and 1200), and clean with (CH3)2CO. Then, clean a few times with bi-distilled water, and dried by soft tissue. Finally, the polishing of sample surface become like a mirror bright, just before immersion in the electrolyte cell.

2.4. Simvastatin Drug as an Inhibitor

The Simvastatin ($\mathbf{C_{25}H_{38}O_5}$) inhibitor has molecular mass (418.566 g/mol), which containing five oxygen atoms, and two π-bonding that act as active centers. The unshared electrons of oxygen atoms, and the electron density of π-bonding acts donor site to the anodic sites of the metal surface.

Copyright © 2020 by Modern Scientific Press Company, Florida, USA



(1S,3R,7S,8S,8aR)-8-(2-((2R,4R)-4-hydroxy-6-oxotetrahydro-2H-pyran-2-yl)ethyl)-3,7,8a-trimethyl-1,2,3,7,8,8a-hexahydronaphthalen-1-yl 2,2-dimethylbutanoate

2.5. Solutions

A stock solution of the Simvastatin was prepared by dissolving 0.0419 gm Simvastatin in one liter [0.5N H_2SO_4 in 10% ethanol-water] to obtain 10^{-4} M Simvastatin solution. This stock solution then diluted by [0.5N H_2SO_4 in 10% ethanol-water] to prepare the desired other solution. These solutions were used as the corrosion medium.

This mixed solution used as a corrosive media, and added the difference of concentrations of the Simvastatin (2, 4, 6, 8 and 10^{-5}) to the corrosive media at different temperatures (15, 25, 35, 45 and 55^{o}C).

2.6. Potentiodynamic Polarization Measurement [23]

Cathodic, and anodic polarization technique was used to determination the rate of corrosion, by using the electrochemical cell that consists of three electrodes:

1) A platinum electrode (as an auxiliary electrode).
2) Calomel electrode (as the reference electrode). ($Hg_{(l)}$ | $Hg_2Cl_{2(s)}$, $KCl_{(aq)}$sat,) E= - 241 mV at 25^{o}C.
3) The working electrode is the LCH sample. The electrolytic cell was filled with 100 ml of the solution, and the sample was immersed in the medium, then the circuit is shorted. The cathodic polarization was firstly measured, and by reverse the current direction the anodic polarization was measured.

2.7. Calculation of the Rate of Corrosion

The anodic, and cathodic polarization was measured by using the over-potential cells. The corrosion current density (I_{corr}), the corrosion potential (E_{corr}), and the corrosion rates (R) are calculated according to the Tafel extrapolation method [24].

Copyright © 2020 by Modern Scientific Press Company, Florida, USA

It is clear that extrapolating the line representing the Tafel region in either cathodic or anodic polarization curve to the corrosion potential will give corrosion current density (I_{corr}), which can be used to calculate the corrosion rate from the equation [25-26].

$$\text{Corrosion rate (mpy)} = 0.1288\ I\ (\text{mA/cm2})\ \text{Eq.wt}\ /d\ (\text{g/cm3}) \quad (1)$$

Where, Corrosion rate (mpy) = mils per year, I = the corrosion current density, d = Specimen density, and, Eq.wt = Specimen equivalent weight.

The corrosion current density (I_{corr}), corrosion potential (E_{corr}), and corrosion rate are recorded in Table 7.

2.8. Applied Evans Technique

The Evans diagrams give good and suitable interpretation of the electrode-electrolyte interface reactions. We can use the following definitions for the items of Evans diagram as follows [27]:

I. $\Delta\phi_{e,m}$ and $\Delta\phi_{e,so}$ are anodic and cathodic potentials at equilibrium at the electrode-electrolyte interface (at I =the exchange current i_o) respectively, where $\Delta\phi e,x = E_{e,x} \pm \left| E_c - E_a \right| i=i_o$; m= metal, so= solution

II. $\Delta\phi = \Delta\phi_{corr}$ = the relative corrosion potential determined from the position of the intersection of the two curves (de-electronation and electronation processes) where I considered as the i_{corr}.

III. The anodic- potential difference at equilibrium (a.p.d,e) $\Delta\phi'_m = \eta_m = \Delta\phi_{corr} - \Delta\phi_{e,m}$.

IV. The cathodic- potential difference at equilibrium (c.p.d,e) $\Delta\phi'_s = \eta_{so} = \Delta\phi_{corr} - \Delta\phi_{e,so}$.

V. The anodic-potential difference (a.p.d) $\Delta\phi'_a = (\Delta\phi_a)_x - (\Delta\phi)_b$; b =bulk, x = with additive, at different concentrations or at different temperatures, and $\Delta I_a = (i)_b - (I)_x$.

VI. The cathodic-potential difference (c.p.d) $\Delta\phi'_c = (\Delta\phi)_b - (\Delta\phi_c)_x$; b=bulk, x= with additive, at different concentrations or at different temperatures, and $\Delta I_c = (i)_b - (I_c)_x$.

These data can be used for kinetic calculations, and to know, which additive is favorable, or which is faster to the electrode surface at the same conditions. It can be used for studying the inhibition mechanism.

2.9. Surface Examinations [28]

The morphology of the LCH surface used for the analysis by examination nature of the surface, and study of changing that appeared on the metal surface. The specimens were prepared by abraded mechanically by using different emery papers up to 1200 grit size and immersed in (10A5H) (blank) then with 10 x 10^{-5}M of Simvastatin at room temperature for one day (24 h). Then, after this immersion time, the specimen was washed gently with distilled water, carefully dried, and take care to the system of surface examinations such as using a scanning electron microscope (SEM), energy dispersive x-ray (EDX), and atomic force microscope (AFM).

Copyright © 2020 by Modern Scientific Press Company, Florida, USA

3. Result and Discussion

3.1. Potentiodynamic Polarization Technique

Study the polarization of the different medium, and with added the various concentrations of Simvastatin as a corrosion inhibitor.

3.11. Dissolution of LCH Sample in 0.5N H_2SO_4 at Different temperatures

Results of the anodic, and cathodic polarization processes for the LCH sample in 0.5N H_2SO_4 at different temperatures in the absence of Simvastatin are shown in Figure 2, and Table 2. It was obvious that the corrosion current density (I_{corr}) is increased as the temperature increased, and the corrosion potential (E_{corr}) is slightly shafted to the more positive value. The polarization processes are started with a potential between about 547, and 553 mV.

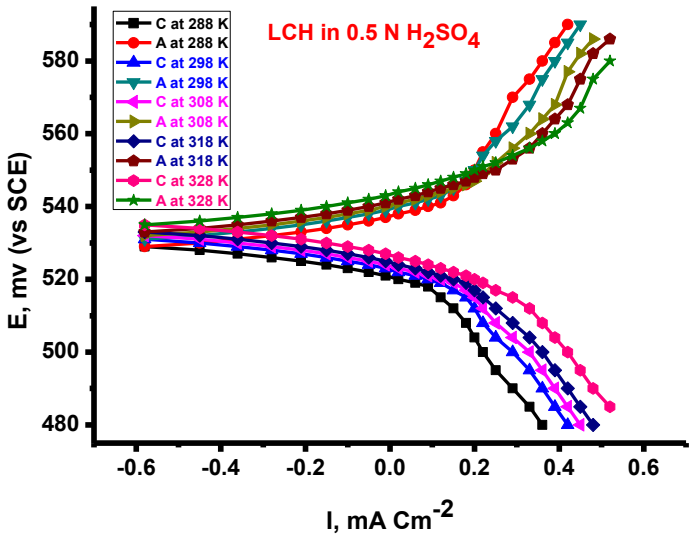


Figure 2: The potentiodynamic polarization curves for corrosion of LCH in 0.5 N of H_2SO_4

The positive potential is increased by anodic polarization, i.e., increase the dissolved component while that the potential decreased by cathodic polarization, i.e., increase the undissolved components. The dissolved component is formed as [29]:

$$Fe \rightarrow Fe^{2+} + 2e$$

$$Fe^{2+} + 2H_2O \rightarrow HFeO^-_2 + 3H^+$$

Where $HFeO^-_2$ Di-hypo-ferrite, green.

In the same time occurs as

$$HFeO_2^- + H^+ \rightarrow Fe(OH)_2$$

Where the undissolved hydrated and the (FeO) can be considered. So that at anodic polarization in the presence of H_2SO_4, the iron is dissolved and formed ferrous sulfate as

$$Fe^{2+} + H_2SO_{4(aq)} \rightarrow Fe\,SO_{4(aq)} + 2H^+$$

Copyright © 2020 by Modern Scientific Press Company, Florida, USA

And the cathodic processes in the presence of H_2SO_4 occurred as

i) $2H^+ + 2e \rightarrow H_2$ hydrogen evolution

ii) $O_{2(g)} + 4H^+_{(aq)} + 4e \rightarrow 2H_2O_{(l)}$ reduced of oxygen

The hydrogen ions adsorbed on the metal surface where an electrochemical reaction takes place in the presence of O_2 as

$M + H_3O^+ + e \rightarrow M{-}H + H_2O$

Where three steps can be done as

a) $2M{-}H \rightarrow 2M + H_{2(g)}\uparrow$

b) $M{-}H + H_3O^+ + e \rightarrow M + H_{2(g)}\uparrow + H_2O$ or

c) $4M{-}H^+ +$ dissolved $O_2 + 4e \rightarrow 4M + 2H_2O_{(l)}$

3.1.2. Dissolution of LCH samples in 10% ethanol at various temperatures[30]

Results of the anodic and cathodic polarization processes for LCH in 10 % ethanol at different temperatures in the absence of Simvastatin are shown in Figure 3, and Table 2. It was obvious that the corrosion current density (I_{corr}) is increased as the temperature increased and the corrosion potential (E_{corr}) is shafted to value that is more positive. The polarization processes are started with a potential between about 278 and 388 mV.

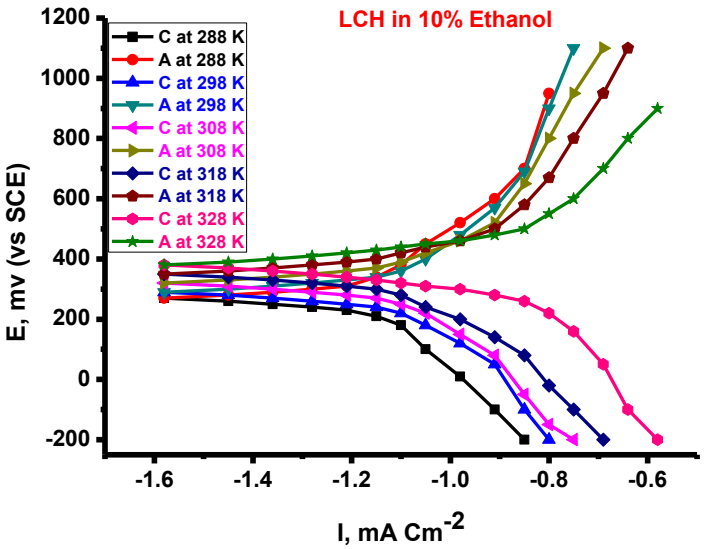


Figure 3: The potentiodynamic polarization curves for corrosion of (LCH) in 10% of ethanol.

The positive potential is increased by anodic polarization, i.e. increase the dissolved component while that the potential decreased by cathodic polarization, i.e., increase the undissolved components. According to the following equation:

$Fe \rightarrow Fe^{2+} + 2e$ anodic reaction

Copyright © 2020 by Modern Scientific Press Company, Florida, USA

$2H_2O + 2e \rightarrow H_{2\,(g)} \uparrow + 2OH^-$ cathodic reaction

In total process:

$Fe + H_2O \rightarrow Fe^{2+} + 2OH^- \rightarrow Fe(OH)_2$

In the bulk the ferrous hydroxide dissolved as

$2Fe(OH)_2 \rightarrow 2FeOH^{++} + 2OH^-$

And,

$2Fe\,OH^{++} + 2e \rightarrow 2Fe\,O + H_2\uparrow$

Table 2: The corrosion potential, corrosion current density and rate of corrosion for (LCH) in 10% ethanol, and 0.5 N H_2SO_4 at various temperatures

Concentration	Temp.	E_{corr}(mV)	I_{Corr}(mA/Cm^2)	Rate (mpy)
10% Ethanol	288K	278	0.08	0.034
	298K	298	0.09	0.038
	308K	328	0.11	0.047
	318K	358	0.12	0.051
	328K	388	0.15	0.064
0.5 N H_2SO_4	288K	547	5.46	2.33
	298K	549	5.53	2.36
	308K	550	5.65	2.41
	318K	551	5.75	2.45
	328K	553	5.90	2.51

3.1.3. Dissolution of LCH in mixed 0.5N H_2SO_4 and 10% ethanol (10A5H)

Results of the anodic, and cathodic polarization processes for (LCH) in mixed solution at different temperatures in the absence of Simvastatin are shown in Figure 4, and Table 6. It was obvious that the corrosion current density (I_{corr}) is increased as the temperature increased, and the corrosion potential (E_{corr}) is shafted to the value that is more positive. The polarization processes are started with a potential between about 538 and 543 mV.

The positive potential is increased by anodic polarization, i.e., increase the dissolved component while that the potential decreased by cathodic polarization, i.e., increase the undissolved components. The results at 288K from Figure 5, and the comparison of I_{corr} in those three media are listed in Table 3.

Copyright © 2020 by Modern Scientific Press Company, Florida, USA

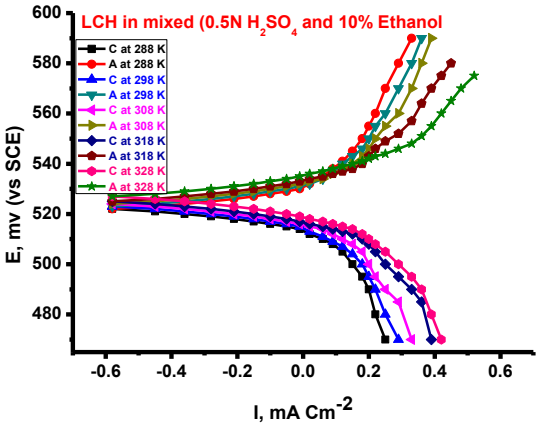


Figure 4: The potentiodynamic polarization curves for the corrosion of LCH in mixed [10A5H] in the nonexistence various concentration of Simvastatin at different temperatures.

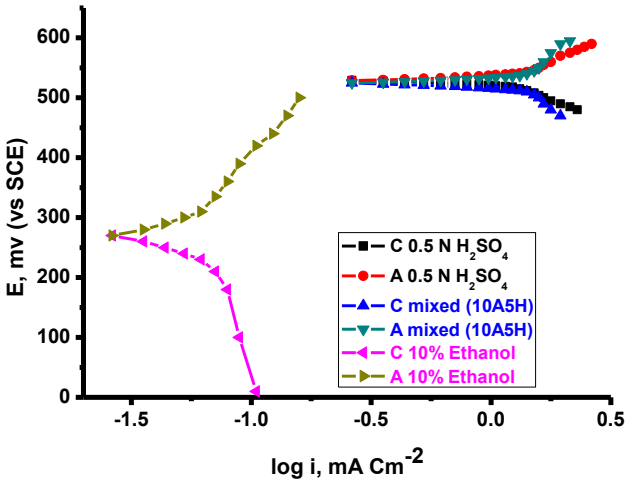


Figure 5: The comparison between the polarization effects in the three mediums of LCH at 288K

Table 3: Comparison between three medium

Corrosive medium	Current density (I_{corr})
	LCH
10% Ethanol	0.08
0.5 N H_2SO_4	5.46
Mixed	4.50

These results concluded that:

a) the corrosion rate in 0.5N H_2SO_4 is very high where the major product is the dissolved component $FeSO_4$ while the formation of undissolved component Fe O is very low and slightly detected, where I_{corr} is rise too (5.46)

b) In the second passivity region (in the presence of 10% ethanol), the undissolved component is considered where the I_{corr} is dropped to (0.08).

Copyright © 2020 by Modern Scientific Press Company, Florida, USA

c) In the presence of a mixed medium, the corrosion rate still very high where I_{corr} is listed (4.50), and the undissolved component can be slightly considered.

3.1.4. Effect of 10% ethanol on the corrosion of steel in 0.5N H_2SO_4 at different temperature

The anodic, and cathodic polarization of the LCH in 0.5N H_2SO_4 with 10 % ethanol at different the temperatures (288, 298, 308, 318 and 328K) are shown in Figure 4.

1) Potentiodynamic polarization technique

In general, as the added 10% ethanol is shifted the potentials to low positive values comparing with only 0.5N H_2SO_4, and both the anodic potential E_a, and the cathodic potential E_c are shifted to low positive values. The anodic current (i_a) slightly decreased (shifted to low values) while the cathodic (i_c) decreased and shifted to low values too, Figures 6 at different temperatures. Values of corrosion potential (E_{corr}), corrosion current density (I_{corr}), and the rate of corrosion in (mpy) are given in Table 6.

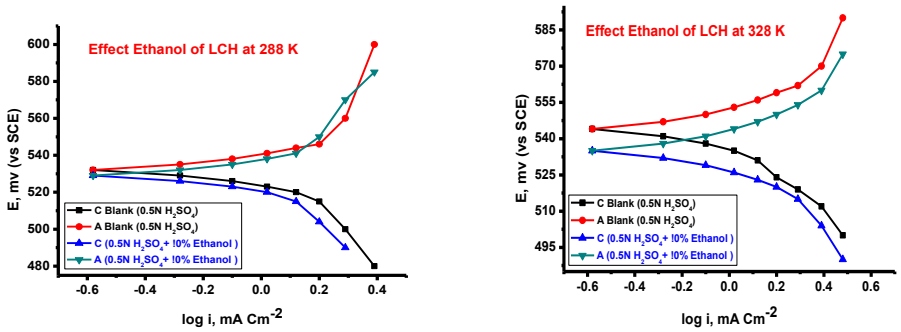


Figure 6: Effect of added 10% ethanol to 0.5N H_2SO_4 on anodic, and cathodic polarization curves of the LCH metal at various temperatures

2) Applied Evans technique

Applying the principle of Evans diagrams in the presence of 10% ethanol with 0.5N H_2SO_4, was drown in Figures7, and the Evans diagram parameters were recorded in the Table4. It is clear that [31]:

The parameters ($\Delta\phi_{corr}$), (i_{corr}), ($\Delta\phi'_m$), ($\Delta\phi'_s$), (α_c), $|\Delta\phi'_c|$, $|\Delta I_a|$, and $|\Delta I_c|$ are slightly increases with increasing the temperatures, but $|\Delta\phi'_a|$ is not clear affect by the increasing temperatures. In the other hand the (α_a), ($\Delta\phi'_a/\Delta I_a$), and ($\Delta\phi'_c/\Delta I_c$) are decreases with increasing the temperatures.

From the results illustrated in Evans diagrams for the electrode- electrolyte interface in (LCH) it is clear that:

The presence of 10% ethanol under polarization technique shifted the de-electronation potential toward the more positive values (positive direction), this means that the polarization oriented of collective ethanol molecules to the electron sink site on the electrode surface, and slow down the metal dissolution. Moreover, the presence of 10%ethanol under polarization technique shifted the electronation potential of acceptor spices to low positive values (negative directions), this means that the collective

Copyright © 2020 by Modern Scientific Press Company, Florida, USA

ethanol molecules are not only adsorbed on the electron sink area, but also the collective ethanol molecules covered the electron source area too. It is clear that, it slowing down (more and more) both the metal dissolution and the hydrogen evolution.

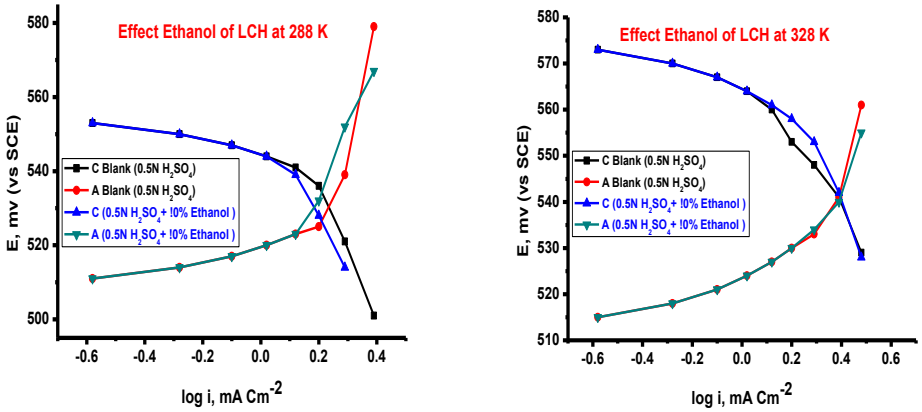


Figure 7: Evans diagrams of the electronation, and the de-electronation potentials vs. log I for the LCH in (10A5H) at various temperatures

Table 4: Relative parameters from Evans diagram of LCH in mixed solutions (10A5H)

Temp.	Δφcorr	Icorr	Δφe,m	Δφe,so	Δφ'm	Δφ's	(i)b	(Δφ)b	(Δφ'a)x	Δφ'a	(Δla)x	Δla*	Δφ'a/Δla	(Δφ'c)x	Δφ'c	(Δlc)x	Δlc	Δφc'/Δl,c	α,a	α,c
288 K	532	1.19	505	545	27	13	1.507	525	534	9	1.21	0.3	30.1	519	6	1.39	0.12	51.28	0.68	0.33
328 K	541	1.59	500	560	41	19	2.344	537	543	6	1.66	0.7	8.772	526	11	1.95	0.39	27.92	0.68	0.32

3.1.5. Effect of add different concentration of Simvastatin inhibitor

The anodic, and cathodic polarization of the LCH in a mixed solution (10A5H) with different concentrations of the Simvastatin (2, 4, 6, 8 and $10x10^{-5}$ M) at 288K are shown in the Figure 8.

1) Potentiodynamic polarization technique

It is obvious that the presence of different concentrations are shifted the potentials to low positive values, both anodic potential E_a, and cathodic potential E_c are shifted to low positive values. The anodic current (i_a) slightly decreased (shifted to low values) while the cathodic (i_c) decreased, and shifted to low values too, that are shown in Figure 9.

The values of the corrosion potential (E_{corr}), the corrosion current density (I_{corr}), and the rate of corrosion in (mpy) are given in Table 6.

Copyright © 2020 by Modern Scientific Press Company, Florida, USA

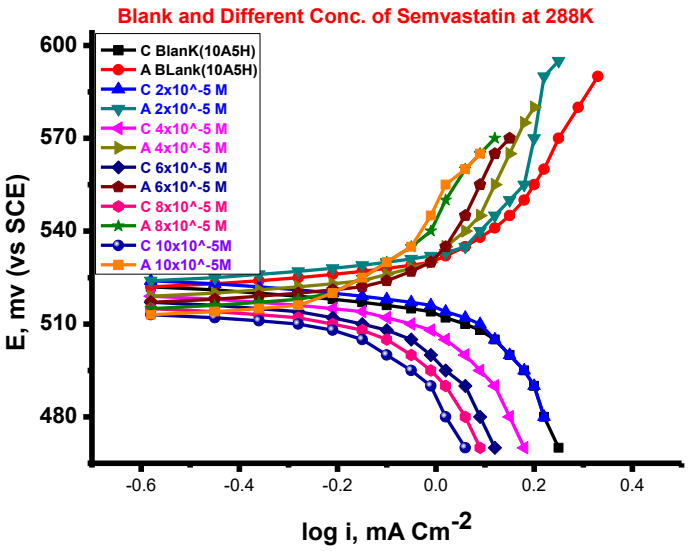


Figure 8: The potentiodynamic polarization curves for the corrosion of the LCH in 10A5H with the existence various concentration of the Simvastatin at 288K.

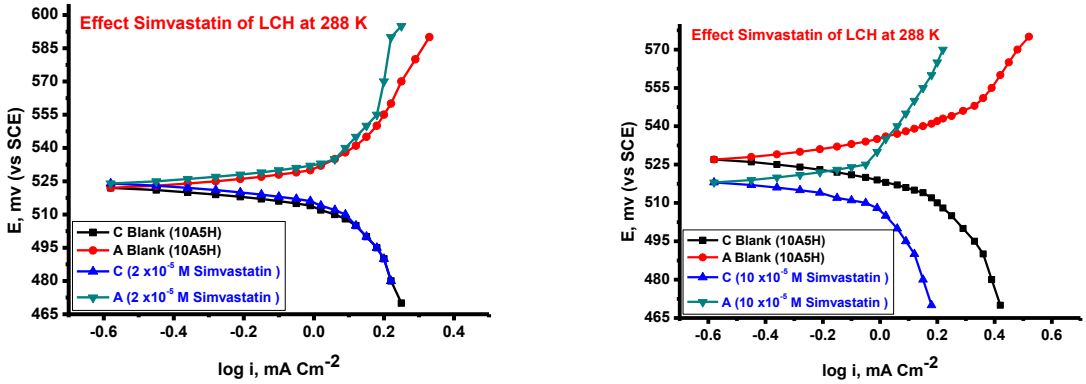


Figure 9: Effect of added the different concentrations of Simvastatin for anodic, and cathodic polarization curves of the LCH metal at 288K

2) Applying Evans technique

Applying the principle of Evans diagrams in the presence of different concentrations from the Simvastatin, which are viewed in Figures 10, and the Evans diagram parameters are listed in Table 5, it is clear that:

The parameters ($\Delta\phi_{corr}$), (i_{corr}), ($\Delta\phi'_m$), (α_a), ($\Delta\phi'_a/\ \Delta I_a$), and ($\Delta\phi'_c/\ \Delta I_c$) are decreases with increasing the temperatures. In the hand the ($\Delta\phi'_s$), (α_c), $|\ \Delta\phi'_a\ |$,$|\ \Delta\phi'_c\ |$, $|\Delta I_a|$, and $|\Delta I_c|$ are increasing with the temperatures increased.

From the above results that illustrated by Evans diagrams for the electrode- electrolyte interface of the LCH. It is clear that:

Copyright © 2020 by Modern Scientific Press Company, Florida, USA

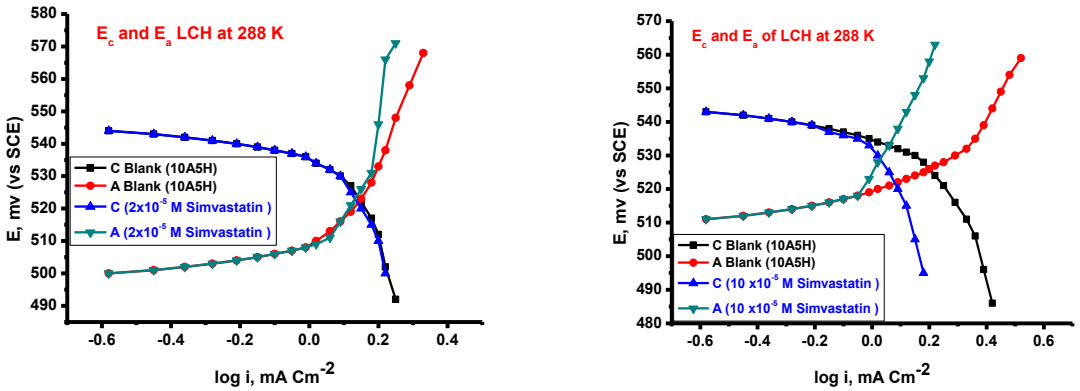


Figure 10: Evans diagrams of the electronation, and the de-electronation potentials vs. log I for LCH with various concentrations of the Simvastatin at 288K.

Table 5: Relative parameters from Evans diagram of LCH with various concentrations of the Simvastatin at 288K

Conc.	Δφcorr	Icorr	Δφe,m	Δφe,so	Δφ'm	Δφ's	(I)b	(Δφ)b	(Δφ'a)x	Δφ'a	(Δla)x	Δla*	Δφ/Δl,a	(Δφ'c)x	Δφ'c	(Δlc)x	Δlc	Δφ'/Δl,c	α,a	α,c
2x10^{-5} M	526	1.38	499	547	27	21	1.514	523	528	5	1.41	0.1	49.5	521	2	1.48	0.03	57.14	0.56	0.44
10x10^{-5} M	522	1	499	547	23	25	1.514	523	536	13	1.1	0.4	31.1	510	13	1.18	0.34	38.35	0.48	0.52

In the presence various concentrations of the Simvastatin under polarization technique. At low Simvastatin concentrations the de-electronation potential shifted toward more positive values (positive direction), this means that the polarization affected the donor functional groups of the Simvastatin molecules, oriented them to the electron sink area on the electrode surface, and slow done the dissolution of the metal. The moderate size of the Simvastatin molecules allow to cover somewhat area of electron source, so that the electronation potential of acceptor spices to low positive value. It is observed that the shifted of the de-electronation potential is larger than the shifted of the electronation potential. In the hand the Simvastatin concentrations increasing the shifted of the electronation potential i.e., the Simvastatin molecules are covered more electron source area on the corroded metal surface with increasing Simvastatin concentrations, and the electronation potential shift is being that the larger than the de-electronation potential shift, which indicating that the slightly formation of multilayer, which adsorbed on the electrode surface. It is clear that the polarization process affects the orientation, and adsorption of the inhibitor molecules, so that both the metal dissolution, and the hydrogen evolution are slowing down more.

Copyright © 2020 by Modern Scientific Press Company, Florida, USA

3.1.6. Effect of temperature on corrosion behavior

The results of the anodic, and cathodic polarization processes for the LCH sample in the corrosive medium are listed in Table 6. The E_{corr}, I_{corr}, and the rate of corrosion were increased with the temperatures increased at the same concentration ($4x10^{-5}$M) of Simvastatin Figure 11.

Table 6: The effect of (Simvastatin) additions on the E_{corr}, I_{corr} and rate of corrosion for (LCH) in (10A5H) at various temperatures

Conc.[I]x 10^5M	Temp. K	E_{corr} (mV)	I_{corr} (mA/Cm^2)	Rate (mpy)	Θ	% IE
0.00	288	538	4.50	1.92	----	----
	298	539	4.60	1.96	----	----
	308	540	4.82	2.06	----	----
	318	541	4.95	2.11	----	----
	328	543	5.20	2.28	----	----
2.00	288	537	1.31	0.56	0.709	70.9
	298	538	1.35	0.58	0.706	70.6
	308	539	1.41	0.60	0.707	70.7
	318	541	1.48	0.63	0.700	70.0
	328	543	1.60	0.68	0.702	70.2
4.00	288	535	1.27	0.54	0.718	71.8
	298	536	1.31	0.56	0.715	71.5
	308	537	1.39	0.59	0.712	71.2
	318	538	1.44	0.61	0.709	70.9
	328	539	1.54	0.65	0.712	71.2
6.00	288	533	1.24	0.53	0.724	72.4
	298	534	1.28	0.55	0.722	72.2
	308	535	1.35	0.58	0.720	72.0
	318	536	1.41	0.60	0.715	71.5
	328	537	1.46	0.62	0.727	72.7
8.00	288	531	1.21	0.51	0.731	73.1
	298	532	1.26	0.54	0.726	72.6
	308	533	1.32	0.56	0.726	72.6
	318	534	1.37	0.58	0.723	72.3
	328	535	1.42	0.61	0.735	73.5
10.00	288	529	1.191	0.51	0.735	73.5
	298	530	1.22	0.52	0.735	73.5
	308	531	1.27	0.54	0.737	73.7
	318	532	1.33	0.57	0.732	73.2
	328	533	1.40	0.60	0.738	73.8

Copyright © 2020 by Modern Scientific Press Company, Florida, USA

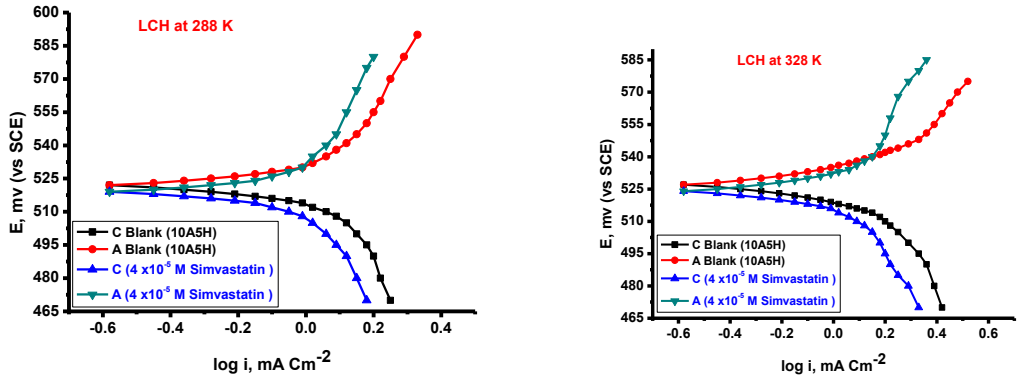


Figure 11: Effect of the temperatures in the presence $4x10^{-5}$M of the Simvastatin on anodic, and cathodic polarization curves of the LCH metal.

3) Potentiodynamic polarization technique

The behavior of the anodic and cathodic polarization indicating that the rate of corrosion of the LCH are stimulated by increasing of the temperature. The increasing of temperatures will be enhance the rate of diffusion of hydrogen (H^+) ion to the metal surface beside the ionic mobility, and increasing the conductivity of the electrolyte. Also, at lower temperatures, absorbed hydrogen atoms which are blocked on the cathodic areas, otherwise the increasing the temperatures of the solution, hydrogen will be disrobed from the cathodic area, i.e., the corrosion rate increased.

4) Apply Evans technique

From the Evans diagrams in the presence of $4x10^{-5}$M Simvastatin, which are viewed in Figures 12, and the Evans diagram parameters are listed in Table 7, it is clear that:

The parameters ($\Delta\phi_{corr}$), ($\Delta\phi'_m$), (α_a), | $\Delta\phi'_c$ |, ($\Delta\phi'_a/\Delta I_a$), and ($\Delta\phi'_c/\Delta I_c$) are decreases with increasing the temperatures. In the other hand (i_{corr}), ($\Delta\phi'_s$), (α_c), | $\Delta\phi'_a$ |, $|\Delta I_a|$, and $|\Delta I_c|$ are increases with increasing the temperatures.

From the results that illustrated in Evans diagrams for the electrode-electrolyte interface it is clear that:

The effect of the temperature on the behavior of the Simvastatin as an inhibitor of the LCH corrosion at $4x10^{-5}$M of Simvastatin. It is obvious that both the electronation, and the de-electronation potentials are shifted to negative and positive direction respectively by increasing the temperature. This behavior clarify that the heat treatment (quenching) divided the electron sink and electron source area to the small parts, so that the size of the Simvastatin sufficient to cover more electron source area be side electron sink.

Copyright © 2020 by Modern Scientific Press Company, Florida, USA

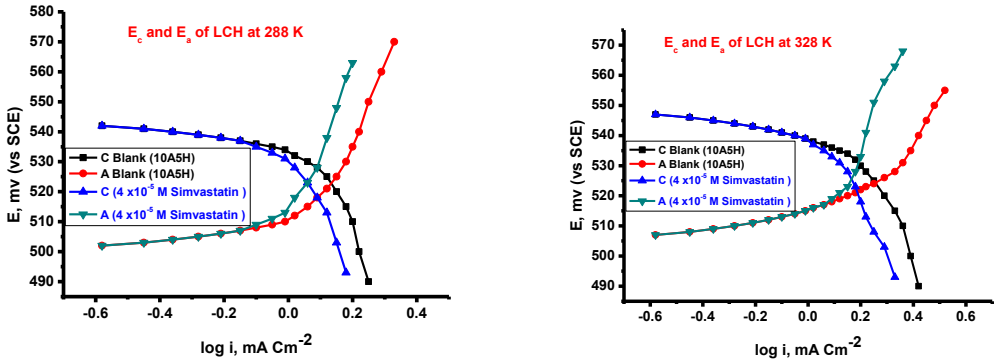


Figure 12: Evans diagrams of the electronation and the de-electronation potentials vs. log I for LCH in the presence of $4x10^{-5}$M of the Simvastatin at various temperatures

Table 7: Relative parameters from Evans diagram of LCH in presence of $4x10^{-5}$M of Simvastatin at various temperatures

Temp.	Δφcorr	Icorr	Δφe,m	Δφe,so	Δφ'm	Δφ's	(i)b	(Δφ)b	(Δφ'a)x	Δφ'a	(Δla)x	Δla*	Δφ/Δl,a	(Δφ'c)x	Δφ'c	(Δlc)x	Δlc	Δφ'/Δl,c	α,a	α,c
288 K	528	1.19	500	544	28	16	1.413	528	530	2	1.26	0.2	12.99	518	10	1.29	0.13	80	0.64	0.36
328 K	526	1.62	497	557	29	31	2.291	521	536	15	1.74	0.6	27.12	515	6	1.89	0.4	14.93	0.48	0.52

3.2. Inhibition efficiency (IE %)

The Simvastatin compound has eight active centers like oxygen atoms an π-bonding act as a donor centers. As a result of the restricted un-plainer structure of the Simvastatin, some active group acts as a donor centers. These centers oriented, and adsorbed on anodic sites (iron carbide), due to the Simvastatin molecule attached with anodic site, and covered somewhat of cathodic area, so that the corrosion rate in the presence of Simvastatin is anodic-cathodic control. The inhibition efficiency (IE %) is calculated as following [32].

$$IE\ \% = [(I_{corr} - I'_{corr})/I_{corr}] \times 100 \quad (1)$$

Where I_{corr}, and I_{corr}' are the corrosion current densities in the absence, and the presence of an inhibitor respectively. The inhibition efficiency data is listed in Table7. It is obvious that the IE % for the LCH sample increases with increasing the Simvastatin concentrations like the following order:

$$10^{-4}>8x10^{-5}>6x10^{-5}>4x10^{-5}>2x10^{-5}\ M$$

Plot IE % against logarithm of the concentrations of Simvastatin inhibitor (log [I]). It is obvious that in the cases 288, 298, 308 and 318K the IE % decreased as the temperature of the medium is increased, but the IE% in 328K increased, this behavior indicated that chemisorption's occurs. See Figure13. The extra part in the curvatures that obtained from polarization technique like S shape

Copyright © 2020 by Modern Scientific Press Company, Florida, USA

indicating that the multilayer proceed from the orientation of functional group under polarization where causes second chemical adsorption over the first layer [33].

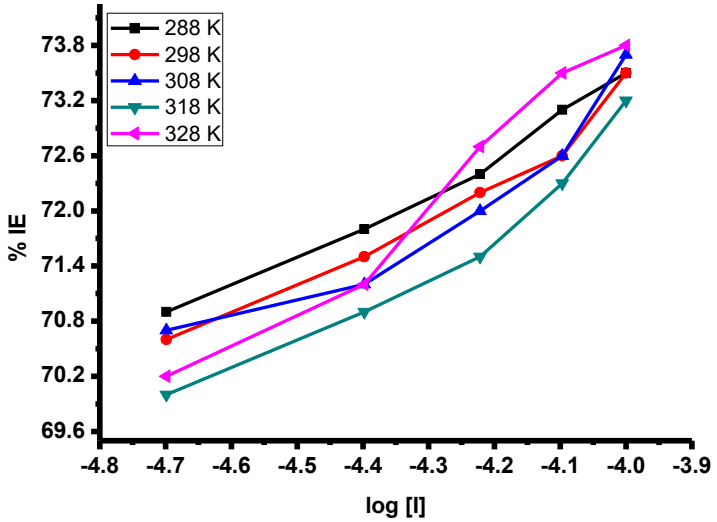
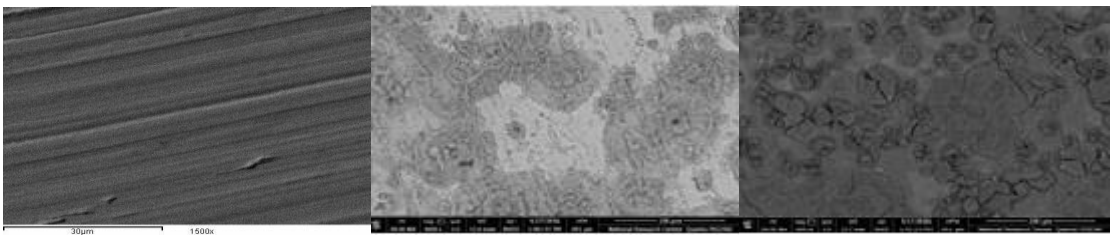


Figure 13: The relation between the IE % and log [I] in (10A5H) for LCH at various temperatures

3.3. Scanning Electron Microscopy (SEM)

The micrographs that obtained for LCH specimens in the nonexistence and in the existence of 10 x 10^{-5}M of Simvastatin drug after exposure for immersion one day in corrosive medium (10A5H). It is clear that LCH is suitable surfaces for corrosion attack in the blank sample or in corrosive medium only Figures 14 a, b and c. When the Simvastatin is existence in the corrosive medium, the morphology of LCH surfaces is quite different from the previous one, and the specimen surface was smoother. It is clear that the formation of a thin film layer adsorbed on the metal surface, which distributed in a disorder way overall surface of the LCH. This may be due to the adsorption of the Simvastatin on the LCH surface and made up the passive film in order to block the active site present on the LCH surface. The Simvastatin molecule interaction with active sites of LCH surface, resulting in a decrease in the contact between LCH and the corrosive medium and sequentially exhibited excellent inhibition effect [34].



a: Free sample (LCH) b: Blank in (10A5H) c: In (10A5H) with existence 10 x 10^{-5}M of Simvastatin

Figures 14: SEM micrographs for LCH in the nonexistence, and the existence of 10 x 10^{-5}M of the Simvastatin after submersion for 1 day

Copyright © 2020 by Modern Scientific Press Company, Florida, USA

3.4. Energy Dispersion Spectroscopy (EDX) [35]

To determination the elements, and molecules that existence or adsorbed on the surface of LCH after one day that immersion in acid with optimum doses of Simvastatin by using the EDX spectra. Figure 15, gives the EDX analysis of LCH in (10A5H) with in the presence of 10 x 10^{-5}M of the Simvastatin. The spectra show additional lines, demonstrating the existence of C (owing to the carbon atoms of some Simvastatin). These data shows that the carbon, nitrogen and oxygen atoms covered the specimen surface. The EDX analysis indicates that only carbon and oxygen are detect and show that the passivation film contained the chemical formula of the Simvastatin drag adsorbed on the surface of the LCH. It is clear that, the percent weight of adsorbed elements C and O were present in the spectra and recorded in Table 8.

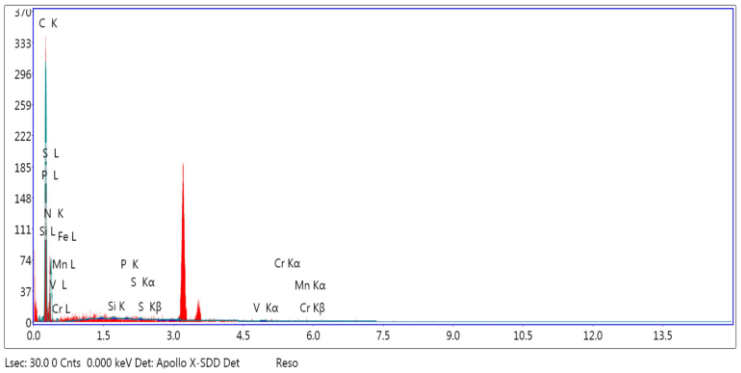


Figure 15: EDS analysis on the LCH in the existence 10 x 10^{-5}M of the Simvastatin drug for 1 day that immersion in (10A5H)

Table 8: Surface composition (wt %) of LCH after one day that immersion in (10A5H) with 10 x 10^{-5}M of the Simvastatin

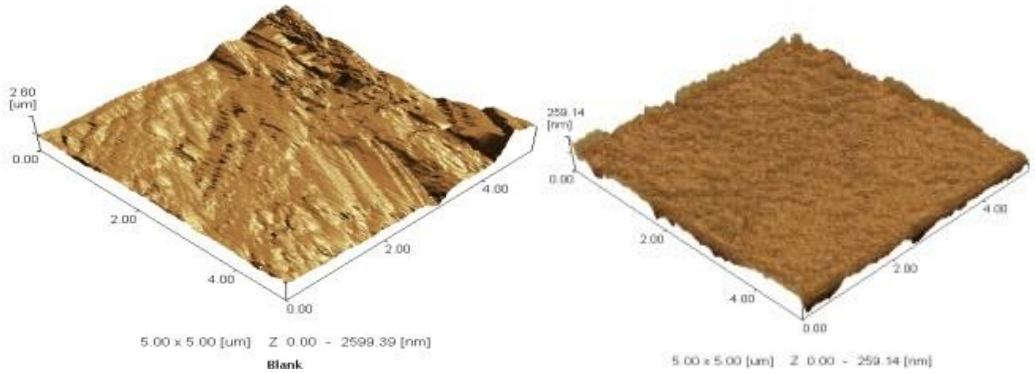
(wt %)	Fe	C	O	N	S	Cl
Simvastatin	62.16	1.32	33.54	1.14	--	1.63

3.5. Atomic Force Microscopy (AFM)

AFM is a powerful tool to investigate the surface morphology of various samples at nano- micro scale that is currently used to study the influence of corrosion inhibitor on the metal solution interface. From the analysis, it can be gained regarding the roughness on the surface. The roughness profile values play an important role to identifying, and report the efficiency of the inhibitor under study. Among the roughness, take a role in explanation about the nature of the adsorbed film on the metal surface [36-37]. Figure 16a, shows the 3D images as well as elevation profiles of polished of the LCH in the absence, and the presence the Simvastatin as an inhibitor. Figure 16b, the surface of LCH specimen (a) exposed to corroded solution affected vales structure with large, and deep crack but the surface (b) reveal that is

Copyright © 2020 by Modern Scientific Press Company, Florida, USA

covering film adsorbed on the metal surface. Conclusion, the adsorption film can protect the surface of the metal from corrosion process. For analysis the values, indicating that the higher value of roughness parameter reached, which found (2.60 µm) for the blank solution which placed in (10A5H) one day and analyzed. The observation of the metal surface which immersed in (10A5H) in the presence of 10 x 10^{-5}M of the Simvastatin as an inhibitor possess small roughness (259.14 nm) compared with the blank solution. It can be noted that the value is lower than that of the blank value. The decrease in the roughness value reflected to the adsorption of inhibitor molecule on metal surface thereby reducing the rate of corrosion.



a: Blank b: In presence 10 x 10^{-5}M of Simvastatin drug

Figure 16: The 3D of optical images of AFM in the nonexistence, and the existence of the Simvastatin drug

3.6. Mechanism of Inhibition

To illustrate the mechanism of inhibition of corrosion on the LCH surface in acid medium by using pharmaceutical drug compound as an inhibitor, it is must be know the nature of metal surface and the nature of the component of inhibitor structure. The LCH is regarded the metal α-phase [38], It is obvious that α-phase state consists of grains and grain boundaries in the surface of the metal, Figure 17. A cross-section of a piece or specimen of the metal that is a corroding to clarify that there are both anodic and cathodic sites in the metal surface structure.

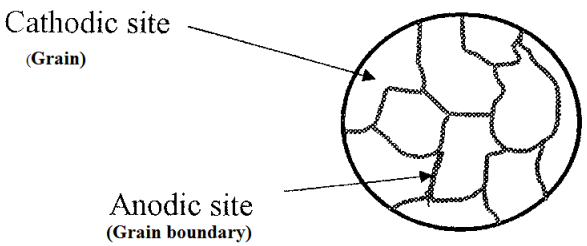


Figure 17: Schema models of metalα- phase

Copyright © 2020 by Modern Scientific Press Company, Florida, USA

The surface of iron is usually, coated with a thin film of iron oxide. However, if this iron oxide film develops some cracks, anodic area are created on the surface, while other metal parts acts as cathodic sets. It follows that the anodic areas are small surface, while nearly the rest of the surface of the metal large cathodes. Electrochemical corrosion involves flow of electric current between the anodic and cathodic areas called inter-granular corrosion. Figure 18, SEM image is shown the corrosion of the LCH in 0.5 N H_2SO_4in one day immersion that illustrated inter-granular corrosion.

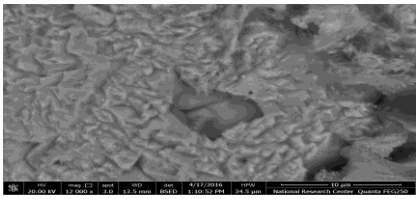


Figure 18: SEM image illustrated inter-granular corrosion after immersion the specimen in 0.5N H_2SO_4one day

All previous results prove that the pharmaceutical drug compound under study were actually inhibit the corrosion of the LCH in 10A5H solution as a corrosive medium. The corrosion inhibition is due to their physical, and chemical adsorption for formation of protection thin film adsorbed on the metal surface. The effect of Simvastatin as inhibitor may be corresponding to the accumulation of the inhibitor molecules on the metal surface, which prevent the direction contact of the metal surface with corrosive environment. The surface of the LCH sample is positively charge in aqueous acid solution and the adsorption occur according to [39-40]:

1) The partial negative charge that present in function group containing Oxygen and electron density of π-bond in Simvastatin may be adsorbed on the positively charge of the metal surface like electrostatic attraction between the opposite charge, in the form of neutral molecules, that involving displacement of water molecules from the metal surface like physical adsorption.
2) The unshared electrons of oxygen atoms and electron density of π bonding donate to the vacant orbital on the metal surface like chemisorption [41].
3) The inhibition action of the inhibitor can be accounted by the interaction between the lone pair of electrons in the O and electron density of π-bond with positively charged (anodic sites) on the metal surface and the skeleton of inhibitor compound cover the cathodic sites this action form thin layer adsorbed on the metal surface and prevent corrosion processes Figure 19.

Copyright © 2020 by Modern Scientific Press Company, Florida, USA

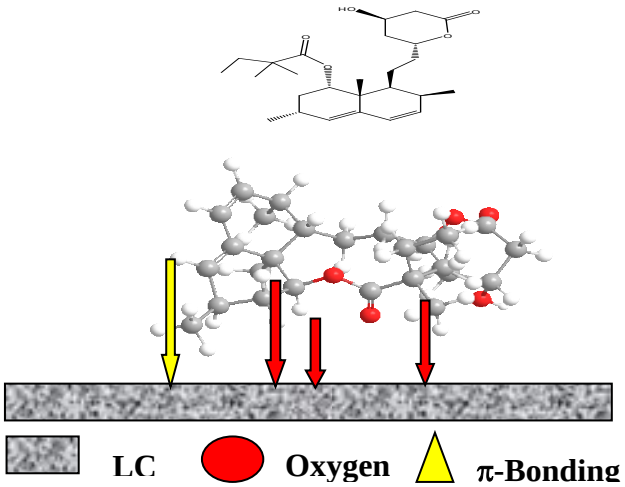


Figure 19: Schema model illustrated the adsorption of the Simvastatin structure on the (LCH) surface.

This meaning, the Simvastatin molecule attached with anodic site and covered somewhat of cathodic area, so that the corrosion rate in presence of Simvastatin is anodic-cathodic control.

4. Conclusion

Inhibition of the corrosion of the LCH in (10A5H) solution by Simvastatin is determine by potentiodynamic polarization, Evans techniques, and surface examination by Scanning Electron Microscopy (SEM), energy Dispersive X-ray (EDX), and atomic force microscopy (AFM). It was found that the inhibition efficiency depends on concentration, nature of metal surface, and the type of adsorption of the inhibitor. The observed corrosion data in the presence the Simvastatin as an inhibitor:

1) The tested Simvastatin inhibitor establish a very good an inhibition efficiency for the LCH corrosion in 10A5H solution
2) Simvastatin inhibit the LCH for the corrosion by the adsorption on its surface and make thin film layer protective them from corrosion process.
3) The inhibition efficiencies of the Simvastatin increases with the increasing of their concentrations.
4) The values of inhibition efficiencies obtained from all techniques that using are seen the validity of the obtained results.
5) The Simvastatin molecule attached with anodic site and covered somewhat of cathodic area, so that the corrosion rate in the presence of the Simvastatin is anodic-cathodic control.

References

[1] Raspini I. A., Influence of Sodium Salts of Organic Acids as Additives on Localized Corrosion of Aluminum and Its Alloys, *Corrosion*, 1993, 49: 821-828.

Copyright © 2020 by Modern Scientific Press Company, Florida, USA

[2] Migahed M. A., Azzam E. M. S., Al-Sabagh A. M. , Corrosion inhibition of mild steel in 1 M sulfuric acid solution using anionic surfactant, *Mater. Chem. Phys*., 2004, 85: 273-279.

[3] Villamil R. F.V., Corio P., Rubim J. C., Siliva M. L., Effect of sodium dodecylsulfate on copper corrosion in sulfuric acid media in the absence and presence of benzotriazole, *J. Electroanal. Chem.*, 1999, 472: 112-119.

[4] Abd El Rehim S. S., Hassan H., Amin M. A., The corrosion inhibition study of sodium dodecyl benzene sulphonate to aluminum and its alloys in 1.0 M HCl solution, *Mater. Chem. Phys.*, 2003, 78, 337-348.

[5] Guo R., Liu T., Wei X., Effects of SDS and some alcohols on the inhibition efficiency of corrosion for nickel, *Colloids Surf., A*, 2002, 209: 37-45.

[6] Branzoi V., Golgovici F., Branzoi F., Aluminum corrosion in hydrochloric acid solutions and the effect of some organic inhibitors, *Mater. Chem. Phys.*, 2002, 78: 122-131.

[7] Elachouri M., Hajji M. S., Salem M., Kertit S., Aride J., Coudert R., Essassi E., Some Nonionic Surfactants as Inhibitors of the Corrosion of Iron in Acid Chloride Solutions, *Corrosion*, 1996, 52:103-108.

[8] Algaber A. S., El-Nemma E. M, Saleh M. M., (2004) Effect of octylphenol polyethylene oxide on the corrosion inhibition of steel in 0.5 M H_2SO_4, *Mater. Chem. Phys.*, 2004, 86: 26-32.

[9] Oukhrib R., El Ibrahimi B., Bourzi H., El Mouaden K., Jmiai A., . El Issami S, Bammou L., Bazzi L., Quantum chemical calculations and corrosion inhibition efficiency of biopolymer "chitosan" on copper surface in 3% NaCl, *JMES*, 2017, 8(1): 195-208.

[10] Al-Azzawi A. M., and Hammud K. K., Newly antibacterial / anti-rusting oxadiazoleporomellitic di-imids of carbon steel / hydrochloric acid interface: Temkin isother model, *IJRPC*, 2016, 6(3): 391-402.

[11] Umar M. Sani1 , Umar Usman, Electrochemical Corrosion Inhibition of Mild Steel in Hydrochloric Acid Medium Using the Antidiabetic Drug Janumet as Inhibitor, *International Journal of Novel Research in Physics Chemistry & Mathematics*, 2016, 3 (3): 30-37.

[12] Kolo A. M., Sani U.M., Kutama U., and Usman U., *The Pharmaceutical and Chemical Journal*, 2016, 3(1): 109-119.

[13] Ameh P. O. and Sani U. M., (2015) Cefuroxime Axetil: A Commercially Available Pro-Drug as Corrosion Drug for Aluminum in Hydrochloric Acid Solution, *Journal of Heterocyclic*, 2015, 1(1): 2-6.

[14] Al-Shafey H. I., Abdel Hameed R. S., Ali F. A., Aboul-Magd A. S., Salah M., (2014) Effect of Expired Drugs as Corrosion Drugs for carbon steel in 1M HCL Solution, *Int. J. Pharm. Sci. Rev. Res.* 2014, 27(1): 146-152.

Copyright © 2020 by Modern Scientific Press Company, Florida, USA

[15] Rupesh Kushwah, Pathak R. K., Inhibition of Mild Steel Corrosion in 0.5 M Sulphuric Acid Solution by Aspirin Drug, *International Journal of Emerging Technology and Advanced Engineering*, 2014, 4 (7): 880-884.

[16] Fouda A. S., EL-Haddad M.N., and Abdallah Y. M., Septazole: Antibacterial Drug as a Green Corrosion Drug for Copper in Hydrochloric Acid Solutions, *IJIRSET*, 2013, 2 (12): 7073-7085.

[17] Ofoegbu S. U. and Ofoegbu P. U., Corrosion inhibition of MS in 0.1 M hydrochloric acid media by chloroquine diphosphate , *ARPN Journal of Engineering and Applied Sciences*, 2012, 7 (3): 272-276.

[18] Kiahosseini S. R., S. Baygi J. M., Khalaj G., Khoshakhlagh A., and Samadipour R., Study on Structural, Corrosion, and Sensitization Behavior of Ultrafine and Coarse Grain 316 Stainless Steel Processed by Multiaxial Forging and Heat Treatment, *Journal of Materials Engineering and Performance*, 2018, 27: 271–281.

[19] Gholamreza K., Mohammad-Javad K., Investigating the corrosion of the Heat-Affected Zones (HAZs) of API-X70 pipeline steels in aerated carbonate solution by electrochemical methods, *International Journal of Pressure Vessels and Piping*, 2016, 145: 1-12.

[20] Narimani N., Zarei B., Pouraliakbar H., Khala G., Predictions of corrosion current density and potential by using chemical composition and corrosion cell characteristics in microalloyed pipeline steels, *Measurement*, 2015, 62: 97-107.

[21] Faizabadi M. J. , Khalaj G. , Pouraliakbar H. and Jandaghi M. R. , Predictions of toughness and hardness by using chemical composition and tensile properties in microalloyed line pipe steels, *Neural Computing and Applications*, 2014, 25: 1993-1999.

[22] Ali Adel H., Corrosion Inhibition of Carbon Steel in Sulfuric Acid By Using N,N –dihydroxy Ethyl Acryl Amide (HEAA) as a New Organic Inhibitor , *International Journal of Modern Chemistry*, 2018, 10 (1): 80-103.

[23] Fouda Abd El-Aziz S., El-Hossiany Ahmed A., Ramadan H. M., Calotropis procera plant extract as green corrosion inhibitor for 304 stainless steel in hydrochloric acid solution, *Zastita Materijala*, 2017, 59 (1): 126 - 140.

[24] Narayan R., *An Introduction to Metallic Corrosion and its Prevention*, Oxford, New Delhi, 1983, p73.

[25] Ailor W. H., *Handbook of Corrosion Testing and Evaluation*, John Wiley &Sons, Inc., New York, 1971, p173-174.

[26] Dacres Sutula C. M., A Larrick B. F., Comparison of Procedures Used in Assessing the Anodic Corrosion of Metal Matrix Composites and Lead Alloys for Use in Lead-Acid Batteries, *Electrochem. Soc*., 1983, 130: 981-985.

Copyright © 2020 by Modern Scientific Press Company, Florida, USA

[27] Crow D. R., *Principles and Applications of Electrochemistry*, Chpman and Hall, London, 3rd ed.. 1988.

[28] Moretti G., Quartanone G., Tassan A., Zingales A., Inhibition of mild steel corrosion in 1N sulphuric acid through indole ,*Wekst. Korros*., 1994, 45: 641-647.

[29] Pourbaix M., *Atlas of Electrochemical Equilibria, In Aqueous Solutions*, Pergamon Press, Oxford, 1966.

[30] Fouda A. S., El- Defrawy A. M., El-Sherbeni M. W., Pharmaceutical compounds as save corrosion inhibitors for CS in 1 M H_2SO_4 solution, *J. Chem*., 2012, 39: 1-27.

[31] Ali Adel H., Electrochemical study for Effect of Gliclazide as a Corrosion Inhibitor of the Carbon Steel in Sulfuric Acid Medium by Applied Potentiodynamic and Evans Techniques, *International Journal of Modern Chemistry*, 2018, 10 (2): 233-255.

[32] Fouda A. S., Al-Sarawy A. A., El-Katori E. E., Pyrazolone derivatives as corrosion inhibitors for Mild steel HCl solution, *Desalination*, 2006, 201: 1-13.

[33] Fouda, A. S., El-Ewady, G., Ali Adel H. Corrosion Inhibition of Carbon Steel in hydrochloric acid medium using gliclazide drug, *Journal for Electrochemistry and Plating Technology*, 2017: 1-20.

[34] Fouda A.S., El-Ewady G., Ali A.H., Modazar as promising corrosion inhibitor of carbon steel in hydrochloric acid solution, *Green Chem. Lett. Rev*., 2017, 10 (2): 88-100.

[35] Fouda A.S., El-Ewady G., Ali Adel H., Corrosion protection of carbon steel by using simvastatin drug in HCl medium, *J. Applicable Chem*., 2017, 6 (5):701-718.

[36] Fouda Abd El-Aziz, S., Ali Adel H., Egy-dronate drug as promising corrosion inhibitor of C-steel in aqueous medium, *Jour. Mater. Prot*., 2018, 59: 126-140.

[37] Ali Adel H., Electrochemical study of candesartan drug as corrosion inhibitor for carbon steel in acid medium, *J. Adv. Electrochem*., (2018) 4 (1): 152-157.

[38] Selim S. R., Review Research to Professor Degree, Interpretation Part Laboratory of Faculty of Science, *Al-Azher University*, 2002, p50.

[39] Solmaz R., Kardas G., Tazc B., Erbil M., Adsorption and corrosion inhibitive properties of 2-amino-5-mercapto-1, 3, 4-thiadiazole on mild steel in hydrochloric acid media, colloids. *Surf. A, physicochem. Eng. Aspects*, 2008, 312: 7-17.

[40] Wahdan M. H., Hermas A. A., Morad M. S., Corrosion inhibition of carbon-steels by propargyltriphenylphosphonium bromide in H_2SO_4 solution, *Mater. Chem. Phys*., 2002, 76: 111-118.

[41] Bentiss F., Trainel M., Gengembre L., A Lagrene M., New triazole derivative as inhibitor of the acid corrosion of mild steel: electrochemical studies, weight loss determination, SEM and XPS, *Appl. Surf. Sci*., 1999, 152: 237-249.

Copyright © 2020 by Modern Scientific Press Company, Florida, USA